Journal of Network and Systems Management (2019) 27:463–488
https://doi.org/10.1007/s10922-018-9474-z

Smart Traffic Offloading with Mobile Edge Computing for Disaster-Resilient Communication Networks

Wen-Pin Chen[1] · **Ang-Hsun Tsai**[2] · **Chung-Hsien Tsai**[3]

Received: 19 October 2017 / Revised: 17 August 2018 / Accepted: 29 August 2018 /
Published online: 8 September 2018

Abstract
When a large-scale natural disaster happens, the evolved node B (eNB) of the disaster area (DA) may be destroyed, and the core network (CN) may be congested with massive data traffic. A disaster-resilient communication system can help relief workers execute the rescue operation. In this paper, we propose a smart traffic offloading mechanism (STOM) on a vehicular eNB (VeNB) to improve the system throughput and delay of the disaster-resilient communication system with heavy CN congestion. Based on the concept of mobile edge computing, the proposed STOM can redirect the traffic flows of relief workers in the same DA to prevent the local data from entering the CN. Therefore, traffic flows between relief workers in the same DA can be transmitted directly through the VeNB only, and system throughput and transmission delay can be significantly improved. Simulation results show that our proposed STOM can achieve 2277% higher system throughput and significantly improve the delay performance, compared with the disaster-resilient communication system without STOM under the worst-case CN congestion environment.

Keywords Rescue operation · Core network congestion · Traffic flows · System throughput · Transmission delay

1 Introduction

Disaster-resilient communication networks can provide communication services for relief workers to share the disaster information in the rescue operation, and for survivors to immediately call for help or report the safety since all the terrestrial communication infrastructure may be destroyed after a strong natural

This work was sponsored by the Ministry of Science and Technology (MOST) of Taiwan under the Grant MOST 107-2221-E-606-005-MY2.

✉ Ang-Hsun Tsai
anghsun@gmail.com

Extended author information available on the last page of the article

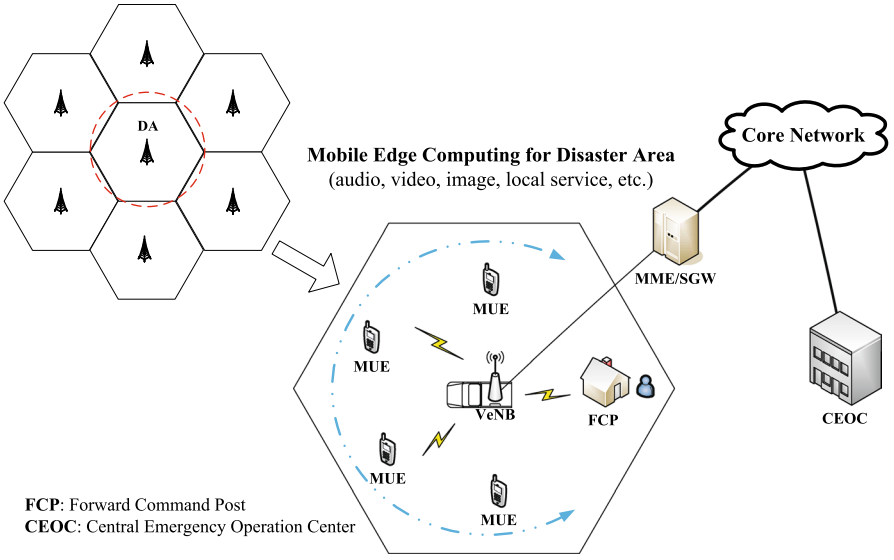

Fig. 1 An illustrative example of a disaster-resilient communication network with the concept of mobile edge computing (MEC)

disaster, such as the East Japan Great Earthquake [1, 2]. In post-disaster periods, the Government organizes a central emergency operation center (CEOC) to direct the rescue operation and arrange the assignment of relief supplies, and many forward command posts (FCPs) are set up in the disaster area (DA) to rescue the survivors and report the disaster information to CEOC, as shown in Fig. 1. The FCP needs to deploy a disaster-resilient communication network to command the relief workers and communicate the disaster information efficiently. With the disaster-resilient communication network, the workers can immediately provide the assistance for discovered survivors, and some undiscovered survivors can try to request the help by themselves. Therefore, a disaster-resilient communication network is very important for an efficient rescue operation.

The core network (CN) may be congested with the traffic (e.g., rescue operation, resident safety confirmation and medical treatment) and the traditional communication service can not support the emergent rescue operation since the data traffic may be increased to eight times larger than the usual in thirty minutes after the disaster [1]. For the traditional communication network, the traffic is always passed into the CN when one worker needs to communicate with another, even if the two workers are in the neighborhood of the same evolved node B (eNB). However, the massive data traffic results in the CN congestion due to the massive demands from the survivors' families and friends. The traditional communication network can not provide the reliable service for the relief workers to do the rescue operation well. In addition, the backhaul to CN is limited because the serious disaster may destroy the terrestrial communication infrastructure, which results in the transmission delay and packet loss. Therefore, an efficient traffic offloading

scheme for the disaster-resilient communication system is the key for success in the rescue operation.

In the literature, some studies on disaster-resilient communication systems focus on the data restoration, such as [3, 4]. In [3], the authors designed a disaster-resilient wireless-link-augmented optical network infrastructure to find the subset of links in an optical network topology for post-disaster recovery. A novel technique [4] for disaster-aware data center placement and content management in cloud networks has been proposed to prevent huge data loss and service disruptions in case of a disaster. However, the papers [3, 4] did not consider the importance of the rescue operation for relief workers. Some papers [5–10] studied the disaster-resilient communication system for relief workers of the rescue operation. The authors in [5] proposed a disaster communication system with key components of Wi-Fi, a satellite link, a GSM system and an LTE base station (BS) to support voice, text and video communication for relief workers and affected citizens who have the demand of safety confirmation for family members and friends. The papers [6, 7] proposed a disaster-resilient communication network architecture based on the integration of satellite and LTE networks to provide a reliable and available backhaul, and to expand coverage of rescue operations. The authors [8, 9] suggested a base station cooperation (BSC) scheme to connect the other BSs out of the DA for backhaul links in the rescue operation. The paper [10] proposed a virtualized evolved packet core (EPC) embedded in eNB and a device-to-device (D2D) communication scheme based on virtualization technology and distributed architecture to improve the resilience ability of the disaster-resilient communication system. However, these papers [5–10] focused on the availability of the framework for the disaster-resilient communication system, and did not consider the situation of low capacity-limited backhaul and CN congestion. Nevertheless, the satellite and the survived BSs in [5–9] only can provide a low capacity-limited backhaul for relief workers and survivors, and may not work immediately after a strong natural disaster. Therefore, a disaster-resilient communication system need some traffic offloading technologies to overcome low capacity-limited backhaul and CN congestion.

Traffic offloading technologies [11], such as local IP access (LIPA) and selective IP traffic offload (SIPTO), have been identified by the Third-Generation Partnership Project (3GPP) as the key solution for the CN congestion. However, the 3GPP only provided a concept, and did not propose an implementation scheme. The paper [12] presented a comprehensive survey of data offloading techniques based on fixed Wi-Fi access points (APs) and terminal-to-terminal (T2T) communications with different considerations of delivery delay guarantees in cellular network system. The authors in [13] proposed different traffic offloading approaches for RAN and CN to help mobile operators solve problems, such as capacity crunch, radio access saturation, average revenues per user decrease, and lack of indoor coverage. Although the CN offloading solutions in [12, 13] can alleviate the congestion situation, the session continuity is still managed by application servers whose locations may be far away from the DA. Therefore, the high demand services for rescue operation should be close to the DA as mobile edge computing (MEC) to support the traffic offloading. The concept of MEC can be used in the CN offloading methods to maintain the session

continuity [14, 15]. For the disaster-resilient communication system, most of rescue information (e.g., relief workers continue searching for survivors and victims, and reporting the research results) are local communication links in the DA. In addition, the MEC enables the cloud computing services to locate at the proximity of the radio access network (RAN) in the DA to reduce the latency of the traffic. The session continuity of the local links on application services can be maintained in the disaster-resilient communication system.

In this paper, we propose a smart traffic offloading mechanism (STOM) based on the concept of MEC to improve the system throughput and delay for the disaster-resilient communication network. After the disaster, the eNB of the DA is assumed to be destroyed, and the FCP deploys a vehicular eNB (VeNB) to replace the original eNB for enhancing the quality of service (QoS) and system throughput in the disaster-resilient communication network. If the CN is congested with the massive traffic after the disaster, the relief workers in the same DA cannot communicate easily with each other under the traditional communication system. With the idea of MEC, the VeNB can offload the traffic between relief workers from the CN, and provide the reliable communication by the STOM. The STOM can help the VeNB determine traffic flows to deliver the CN or redirect to the other relief workers in the same DA based on the destination of the transmitted packets. Therefore, traffic flows between relief workers within the same DA do not pass through the CN congested by the other massive traffic flows from the other eNBs, and the transmission delay and system throughput of this disaster-resilient communication network is improved. The simulation results show that our proposed STOM can help the disaster-resilient communication system improve throughput by 2277% and save huge transmission time compared to the disaster-resilient communication system without STOM under the worst-case CN congestion environment (i.e., the CN network capacity is left mere one Mbps with ten users).

The main contributions of this paper are summarized as follows:

- This paper investigates the impact of CN congestion on system throughput and transmission delay while considering both RAN and CN capacities in the disaster-resilient communication system.
- We propose a suitable disaster-resilient communication system architecture with MEC concept to achieve the objective of traffic offloading for both data flows and application services.
- We adopt the MEC technology in the disaster-resilient communication system to avoid the CN congestion and to significantly improve system throughput and transmission delay.
- The proposed STOM allows disaster-resilient communication systems to efficiently support rescue operations within the DA.

The remainder of this paper is organized as follows: Sect. 2 introduces the system model, including the disaster relief scenario, channel model, traffic flow, and performance metrics. The proposed STOM is detailed in Sect. 3, and the

simulation results are shown in Sect. 4. Finally, we give the concluding remarks in Sect. 5.

2 System Model

2.1 System Architecture

Figure 1 shows the illustration of a disaster-resilient communication network with the concept of the mobile edge computing (MEC). The rescue operation has two main transmission types for disaster communications in our scenario. The relief workers inside the DA can communicate with each other for rescuing the survivors. The FCP also can communicate with CEOC outside the DA for reporting the disaster information and requesting supports. Therefore, we assume that the original terrestrial cellular communication system of the DA is destroyed by the natural disaster, and the FCP with one VeNB is deployed in the DA to provide the disaster-resilient communication service for relief workers to execute the rescue operation. In this paper, we define the relief workers as the mobile user equipments (MUEs) of the VeNB inside the DA. The VeNB can connect to the CN with a wire link by passing the mobility management entity (MME) and serving gateway (SGW) so that the CEOC can control the rescue operation. The N_{MUE} MUEs as well as the FCP are located uniformly within the DA, and can share the disaster information with each other through the VeNB. In addition, we assume that N^*_{MUE} users are uniformly located in the other macrocells (eNBs) surrounding the DA, as shown in Fig. 1. Therefore, the MUEs of the DA may suffer the interference from the other eNBs in the downlink. For the effect of nature disaster, we assume that the CN is congested with the massive data traffic, such as rescue operation, resident safety confirmation, medical treatment, etc.

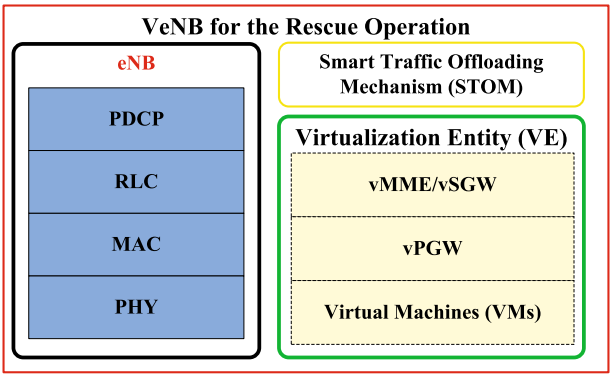

Fig. 2 An illustrative components of VeNB with the concept of mobile edge computing (MEC), including a conventional eNB module and the proposed STOM and VE modules

2.2 VeNB Modules with MEC

We introduce the proposed VeNB with MEC concept for the rescue operation. As shown in Fig. 2, the proposed VeNB consists of the conventional eNB module, the smart traffic offloading mechanism (STOM) module, and the virtualization entity (VE) module. The VeNB can provide MEC services (e.g., the applications of rescue operation) for mobile subscribers in the proximity of VeNB [15–19] to increase the rescue efficiency. The eNB module has the existing user plane protocol stacks [20], including the packet data convergence protocol (PDCP), the radio link control (RLC), the media access control (MAC), and the physical (PHY). The VE module has three virtualized components, including the virtual-MME/SGW (vMME/vSGW), the virtual packet data network gateway (vPGW), and the virtual machines (VMs) with local application services. The vMME/vSGW can manage the subscription information and mobility of relief workers, and can forward users' data packets to the vPGW. The vPGW can provide the connectivity between the MUE and various VMs which are major application servers for the rescue operation.

For conventional cellular communication networks, the data transfer from a MUE to an another MUE has to pass through the CN (i.e., EPC), even if the two MUEs are in the proximity or in the same service region of the eNB. However, with the deep packet inspection (DPI) for the data, the STOM realizes the IPs of source and destination, and can determine the suitable traffic link from the eNB module for MUEs according to the type of service (ToS). If the data has to be processed by a general application server in the far area, the STOM can pass the data through the CN to the server. The STOM can pass the data through the VE to the virtual machines (VMs) in the same VeNB, if the data has to be processed by the rescue application server. Additionally, the STOM can redirect the data through the original eNB module to the other MUEs in the same VeNB region, if the purpose of the data is only for transmission. Therefore, the system throughput and transmission delay can be significantly improved, as well as the rescue efficiency.

2.3 Channel Model

Different from the wired communication with a fixed transmission path and a stable transmission medium, the wireless communication signal attenuates seriously on transmission due to the path loss, reflection, diffraction, scattering, etc. Therefore, we must consider the channel effects of large-scale fading and small-scale fading. The large-scale fading is composed of path loss and shadowing effect. The path loss effect is caused by the distance between the transmitter and receiver, while the shadowing effect is caused by the obstacles in the transmission path. The small-scale fading is considered as the frequency-selective multipath fading for scheduling. In this paper, we consider the effects of path loss, shadowing, and frequency-selective multipath fading on the channel model, which are detailed as follows.

2.3.1 Path Loss

For a cellular system, the path loss between the transmitter and the receiver with a propagation distance d (km) is defined as [21].

$$L_{dB}(d) = 127 + 30\log_{10}(d). \tag{1}$$

2.3.2 Shadowing

Shadowing is modelled by a log-normal random variable $10^{X_{SF}}$, where $X_{SF} \in N\left(0, \xi^2\right)$ is the Gaussian distributed random variable with zero mean. The standard deviation for cellular links shadowing is $\xi = 8$ dB.

2.3.3 Frequency-Selective Multipath Fading

The Rayleigh fading channel h is considered as the frequency-selective multipath fading channels in this paper. With the frequency-selective multipath fading channels, the eNB can schedule the radio resource for users. In the LTE standard [21], a resource block (RB) is the smallest channel bandwidth to be scheduled by eNB for transmission. In this paper, we consider the round robin scheduling to allocate the RBs to MUEs for the VeNB in the disaster-resilient communication network. With the round robin scheduling, the MUEs can in term select the optimal channels for transmission. In addition, the fairness among MUEs can be achieved.

2.3.4 Received Power Strength

The wireless communication signal may attenuate seriously during transmission due to the channel effect. For a receiver, the received power strength from a transmitter is effected by the path loss, shadowing, and frequency-selective multipath fading. With the large-scale fading and small-scale fading, the received power strength S_r from a transmitter to a receiver can be modelled as

$$S_r = \frac{P_t \cdot 10^{X_{SF}/10} \cdot |h|^2}{10^{L_{dB}(d)/10}}, \tag{2}$$

where P_t is the transmission power of the transmitter, X_{SF} is the log-normal shadowing effect, h is the Rayleigh fading channel gain, and $L_{dB}(d)$ represents the impact of path loss.

2.4 Traffic Flows

For the rescue operation, the traffic flows (e.g., audio, video, image and text) are generated by a source (i.e., a relief worker) and be transferred to a destination (i.e., another relief worker). Because these traffic flows may pass the RAN and

CN, the capacities of RAN and CN are the key factors to improve the performance of the disaster-resilient communication system, as detailed in the following.

2.4.1 Data Generation

We assume that each MUE randomly generates the traffic data with the maximum data generation rate $R_{traffic}$ and transmits simultaneously at the same transmission time interval (TTI) during the rescue time. Denote $\eta_{k,k',t}$ as the data bit generated by the k'-th MUE to transmit to the k-th MUE at the t-th TTI in the DA during the rescue time period T, where $k, k' = 1, 2, \ldots, N_{MUE}, k \neq k'$ and $t = 1, 2, \ldots, T$. Therefore, these data can be transferred from a source (i.e., a MUE or the FCP) to a destination (i.e., another MUE or the FCP) with delays according to the capacities of RAN and CN.

2.4.2 Routing Paths

For the conventional disaster-resilient communication network, the information is generated by a source and is transferred to a destination through the VeNB, the SGW, and the CN, as shown in Fig. 3. To explain the routes, we assume that each MUE (including FCP), the VeNB, the SGW, and the CN has the respective buffer, and can be divided into uplink buffer and downlink buffer. The uplink buffer and the downlink buffer can transfer the data through the uplink route and the downlink route, respectively. The uplink route represents that the data is transferred from the MUE to the CN through the VeNB and the SGW, while the downlink route implies that the data is transferred from the CN to the MUE through the SGW and the VeNB.

For the rescue operation, we assume that the buffer capacity is large enough to accommodate all the transferred traffic flows. Therefore, we assume that the

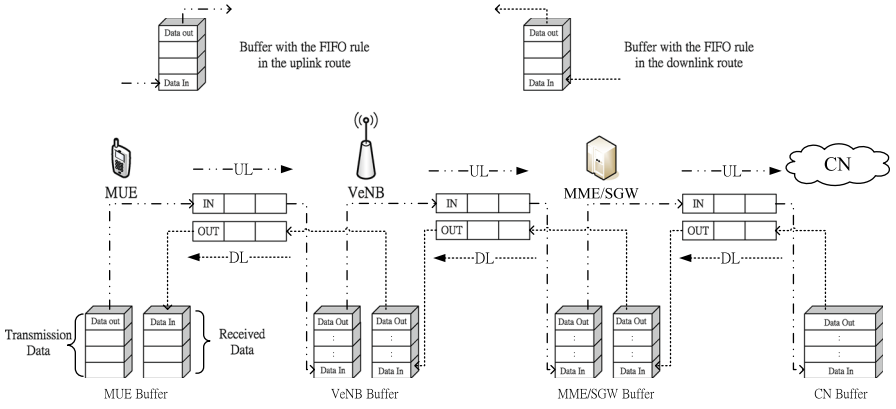

Fig. 3 Traffic flows with buffers of the MUE, VeNB, SGW, and CN entities for the conventional communication network

buffer delay is short enough to be neglected. Moreover, the buffer queueing follows the first in first out (FIFO) rule.

2.4.3 RAN Capacity

The RAN capacity for data transmission comprises uplink and downlink phases. For uplink, the signal-to-interference-plus-noise-ratio (SINR) of the k-th MUE on the n-th RB is denoted as $SINR^{UL}_{n,k}$, and can be defined as

$$SINR^{UL}_{n,k} = \frac{S^{UL}_{n,k}}{\sum_{k^*,k^* \neq k} S^{UL}_{n,k^*} + N_0}, \tag{3}$$

where $S^{UL}_{n,k}$ is the received signal power of the n-th RB from the k-th MUE to the VeNB, and S^{UL}_{n,k^*} is the interference from the other MUE of the neighboring eNB. N_0 is the power spectrum density of AWGN.

Similarly, the downlink SINR of the k-th MUE on the n-th RB in the i-th VeNB is denoted as $SINR^{DL}_{n,k,i}$, and can be defined as

$$SINR^{DL}_{n,k,i} = \frac{S^{DL}_{n,k,i}}{\sum\limits_{j,j \neq i} S^{DL}_{n,k,j} + N_0}, \tag{4}$$

where $S^{DL}_{n,k,i}$ is the received signal power of the n-th RB from the i-th VeNB to the k-th MUE, and $S^{DL}_{n,k,j}$ is the interference from the other eNBs of the neighboring eNB.

According to Shannon's formula, the UL and DL capacity of the k-th MUE can be respectively expressed as

$$C^{UL}_k = \sum_{n=1}^{N_{RB}} B_{RB} \log_2 \left(1 + SINR^{UL}_{n,k}\right), \tag{5}$$

$$C^{DL}_k = \sum_{n=1}^{N_{RB}} B_{RB} \log_2 \left(1 + SINR^{DL}_{n,k,i}\right), \tag{6}$$

where N_{RB} is the number of RBs, and B_{RB} is the bandwidth of a RB.

2.4.4 CN Capacity

The CN capacity contains the transmission rate of the buffer and the data propagation rate over the wire links. We define the transmission rate of a buffer as $R_{transmission}$ to estimate the data transfer time between the buffer and the physical interface, and

data propagation rate as $R_{propagation}$ to evaluate the propagation time between VeNB and SGW and between the SGW and the CN. In general, $R_{transmission} \gg R_{propagation}$, so we define the CN capacity limitation as $R_{propagation}$.

2.4.5 Data Received

During the rescue time period T, each MUE can receive many data with corresponding transmission time from the other MUEs. Assume that the k-th MUE receives the μ-th data packet with $\rho_{k,\mu}$ bits and the corresponding transmission time $\Delta t_{k,\mu}$ from the the corresponding transmission MUE (i.e., the source).

2.5 Performance Metrics

The average throughput of the k-th MUE can be defined as

$$R_k = \frac{1}{\beta_k} \sum_{\mu=1}^{\beta_k} \frac{\rho_{k,\mu}}{\Delta t_{k,\mu}} , \tag{7}$$

where β_k is the amount of data received by the k-th MUE during the rescue time period T. Therefore, the total system throughput can be defined as

$$\Gamma = \sum_{k=1}^{N_{MUE}} R_k = \sum_{k=1}^{N_{MUE}} \frac{1}{\beta_k} \sum_{\mu=1}^{\beta_k} \frac{\rho_{k,\mu}}{\Delta t_{k,\mu}} . \tag{8}$$

The transmission delay of the k-th MUE can be defined as

$$t_k = \frac{1}{\beta_k} \sum_{\mu=1}^{\beta_k} \Delta t_{k,\mu} , \tag{9}$$

and the average transmission delay can be defined as

$$D = \frac{1}{N_{MUE}} \sum_{k=1}^{N_{MUE}} t_k = \frac{1}{N_{MUE}} \sum_{k=1}^{N_{MUE}} \frac{1}{\beta_k} \sum_{\mu=1}^{\beta_k} \Delta t_{k,\mu} . \tag{10}$$

3 Smart Traffic Offloading Mechanism (STOM)

This section introduces smart traffic offloading with MEC that can minimize the average delay to obtain the maximum average system throughput. The STOM and VE modules are implemented in VeNB to minimize the number of data transmission paths, particularly in both the backhaul and the CN. Eliminating unnecessary

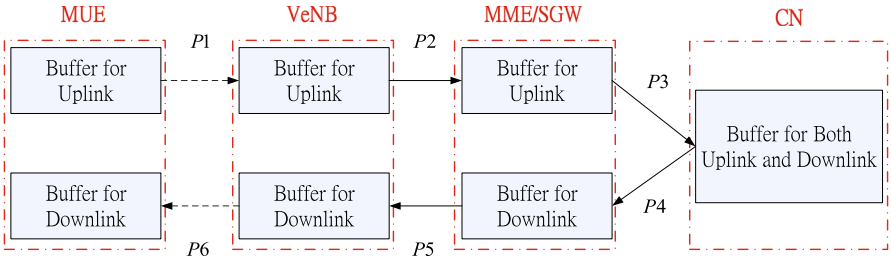

Fig. 4 An illustrative of transmission data path between each entity

data transmission paths can reduce the probability of packet loss, the data processing delay, and the queuing delay. Thus, both the reliability and the performance of disaster-resilient communication systems are improved significantly.

In general, the data packets are generated by a MUE and propagated to another MUE through the network entities, such as VeNB, MME/SGW, and CN. As shown in Fig. 4, we define the paths from the MUE to VeNB, from VeNB to MME/SGW, from MME/SGW to CN, from CN to MME/SGW, from MME/SGW to VeNB, from VeNB to the other MUE as $P1$, $P2$, $P3$, $P4$, $P5$, and $P6$, respectively. Denote $\Delta t_{k,\mu}^{P1}$, $\Delta t_{k,\mu}^{P2}$, $\Delta t_{k,\mu}^{P3}$, $\Delta t_{k,\mu}^{P4}$, $\Delta t_{k,\mu}^{P5}$, and $\Delta t_{k,\mu}^{P6}$ as the transmission time of the μ-th data for the k-th MUE on $P1$, $P2$, $P3$, $P4$, $P5$, and $P6$, respectively. In addition, the STOM with the DPI can realize the IPs of the source and the destination. Different from the normal transmission mode, the STOM mode has additional DPI time for packet processing. Denote $t_{k,\mu}^{DPI}$ as the DPI time of the μ-th data for the k-th MUE on the VeNB.

For RAN, $P1$ and $P6$ imply the uplink and downlink paths, and the data transmission time $\Delta t_{k,\mu}^{P1}$ and $\Delta t_{k,\mu}^{P6}$ depend on the RAN capacity. Thus, for the μ-th data of the k-th MUE, the transmission time of $P1$ and $P6$ can be expressed as

$$\Delta t_{k,\mu}^{P1} = \frac{\rho_{k,\mu}}{C_k^{UL}}, \tag{11}$$

$$\Delta t_{k,\mu}^{P6} = \frac{\rho_{k,\mu}}{C_k^{DL}}. \tag{12}$$

For CN on $P2$ and $P5$, the data transmission time $\Delta t_{k,\mu}^{P2}$ and $\Delta t_{k,\mu}^{P5}$ can be estimated based on the transmission rate of the buffer $R_{transmission}$ and the data propagation rate $R_{propagation}$ between the VeNB and MME/SGW. While the data transmission time $\Delta t_{k,\mu}^{P3}$ and $\Delta t_{k,\mu}^{P4}$ can be determined by the transmission rate of a buffer $R_{transmission}$ and the data propagation rate $R_{propagation}$ between the MME/SGW and CN for $P3$ and $P4$.

$$\Delta t_{k,\mu}^{P2} = \Delta t_{k,\mu}^{P5} = \left\lceil \frac{\rho_{k,\mu}(\text{VeNB} \rightleftharpoons \text{MME/SGW})}{R_{transmission}} \right\rceil + \left\lceil \frac{\rho_{k,\mu}(\text{VeNB} \rightleftharpoons \text{MME/SGW})}{R_{propagation}} \right\rceil, \tag{13}$$

$$\Delta t_{k,\mu}^{P3} = \Delta t_{k,\mu}^{P4} = \left\lceil \frac{\rho_{k,\mu}(\text{MME/SGW} \rightleftharpoons \text{CN})}{R_{transmission}} \right\rceil + \left\lceil \frac{\rho_{k,\mu}(\text{MME/SGW} \rightleftharpoons \text{CN})}{R_{propagation}} \right\rceil, \tag{14}$$

where $\lceil x \rceil$ is the ceiling function that maps x to the least integer.

With the DPI technology, the STOM module in the VeNB can realize not only general information of data packets (e.g., the source IP, destination IP, source port, destination port, etc.), but also the advanced information about application services and GPRS tunnelling protocol user plane (GTP-U) tunnels. Because the GTP-U header is arranged with the outer layer of data packet and comprises the information of tunnel endpoint ID (TEID) and IP address pairs [22], the STOM module can inspect the data packet and intelligently determine the optimal transmission path for this data packet. In this paper, three formats of GTP-U headers are assumed with the data packet and can be denoted as H_{SGW}, H_{vSGW} and H_k. The GTP-U header H_{SGW}, H_{vSGW}, and H_k can tell the STOM module the routing paths from eNB module to the SGW, the vSGW module, and the k-th MUE, respectively.

For the data packet $\rho_{k,\mu}$, the STOM module can do the DPI to know the ToS (S), source IP (IP_S), destination IP (IP_D), and payload (ψ) (i.e., the amount of transferred data bits). For the sake of simplicity, we define a data structure $\Omega_{k,\mu}$ to include the necessary information that can be processed by the STOM module, and $\Omega_{k,\mu} = \{\text{GTP-U header}, S, IP_S, IP_D, \psi\}$. In addition, we assume that the ToS (S) includes data packet transmission mode (S_ϕ) and application service transmission mode (S_θ). Moreover, we build a served MUE IP table Ψ for the STOM module to collect the IP information of relief workers in the same VeNB.

When the μ-th data packet $\rho_{k,\mu}$ is generated by the k-th MUE, the data would be transmitted to VeNB. After receiving the data packet $\rho_{k,\mu}$, the VeNB can realize the information of data structure $\Omega_{k,\mu}$ by the DPI of the STOM. The information of data structure $\Omega_{k,\mu}$ includes the GTP-U header, the ToSs (S), source IP (IP_S), and the destination IP (IP_D). With the information of data structure $\Omega_{k,\mu}$, the STOM can keep or replace the GTP-U header to route the data packet $\rho_{k,\mu}$ to the node of destination. Generally, the ToS (S) of data structure $\Omega_{k,\mu}$ has two kind of modes. One is the data packet transmission mode (S_ϕ), and the other is the application service transmission mode (S_θ). For the two modes, the STOM can decide the next node as inside or outside the DA according to the MUE IP table Ψ. If both source IP (IP_S) and destination IP (IP_D) are in the MUE IP table Ψ, the data packet $\rho_{k,\mu}$ belongs to the relief workers inside the DA. The STOM replaces the existing GTP-U header H_{SGW} with H_k and H_{vSGW} of data structure $\Omega_{k,\mu}$ for data packet transmission mode (S_ϕ) and the other is the application service transmission mode (S_θ), respectively. According the new data structure $\Omega_{k,\mu}$, the data packet $\rho_{k,\mu}$ can be redirected to the MUE inside the DA by the VeNB. On the contrary, the data packet $\rho_{k,\mu}$ does not belong to the relief workers inside the DA if both source IP (IP_S) and destination IP (IP_D) are not in the MUE IP table Ψ. Therefore, the STOM keeps the existing GTP-U header of data structure $\Omega_{k,\mu}$, and the VeNB forwards the data packet $\rho_{k,\mu}$ to the MME/SGW entity. The STOM algorithm is described as Algorithm 1.

Algorithm 1 Smart traffic offloading mechanism (STOM)

Input:
The input data packet $\rho_{k,\mu}$ and the served MUE IP table Ψ.
Output:
The output data packet $\rho_{k,\mu}$.
Pseudo-code:

Do the DPI for the data packet $\rho_{k,\mu}$ and obtain the data structure $\Omega_{k,\mu}$.
$\Omega_{k,\mu} = \{H_{SGW}, S, IP_S, IP_D, \psi\}$.
if $S = S_\phi$ **then**
  $\Omega_{k,\mu} = \{H_{SGW}, S_\phi, k', k, \psi\}$.
  if $k \in \Psi$ **then**
    Replace H_{SGW} with H_k.
    $\Omega_{k,\mu} = \{H_k, S_\phi, k', k, \psi\}$.
    Redirect the data packet $\rho_{k,\mu}$ to the k-th MUE in the VeNB.
  else
    Keep the GTP-U header H_{SGW} for $\Omega_{k,\mu}$.
    $\Omega_{k,\mu} = \{H_{SGW}, S_\phi, k', k, \psi\}$.
    Forward the data packet $\rho_{k,\mu}$ to the MME/SGW entity.
  end if
else $S = S_\theta$
  $\Omega_{k,\mu} = \{H_{SGW}, S_\theta, k', k, \psi\}$.
  if $k \in \Psi$ **then**
    Replace H_{SGW} with H_{vSGW}.
    $\Omega_{k,\mu} = \{H_{vSGW}, S_\theta, k', k, \psi\}$.
    Redirect the data packet $\rho_{k,\mu}$ to the vMME/vSGW module.
  else
    Keep the GTP-U header H_{SGW} for $\Omega_{k,\mu}$.
    $\Omega_{k,\mu} = \{H_{SGW}, S_\theta, k', k, \psi\}$.
    Forward the data packet $\rho_{k,\mu}$ to the MME/SGW entity.
  end if
end if

Conventionally, the transmission data should be sequentially passed through $P1$, $P2$, $P3$, $P4$, $P5$, and $P6$, even if the source MUE and the destination MUE are in the same cell coverage. However, the proposed STOM can route the transmission data through the optimal path $P1$ and $P6$, when the transmission and received relief workers are served by the same VeNB. Therefore, for the μ-th data received by the k-th MUE, the transmission delay can be $\Delta t_{k,\mu}^{Normal}$ and $\Delta t_{k,\mu}^{STOM}$ with the normal transmission scheme and the STOM transmission scheme, respectively. The transmission delay $\Delta t_{k,\mu}^{Normal}$ and $\Delta t_{k,\mu}^{STOM}$ are expressed as

$$\begin{aligned}\Delta t_{k,\mu}^{Normal} = \Delta t_{k,\mu}^{P1} + \Delta t_{k,\mu}^{P2} + \Delta t_{k,\mu}^{P3} \\ + \Delta t_{k,\mu}^{P4} + \Delta t_{k,\mu}^{P5} + \Delta t_{k,\mu}^{P6},\end{aligned} \tag{15}$$

$$\Delta t_{k,\mu}^{STOM} = \Delta t_{k,\mu}^{P1} + t_{k,\mu}^{DPI} + \Delta t_{k,\mu}^{P6}. \tag{16}$$

For the μ-th data received by the k-th MUE, the system throughput is Γ^{Normal} and Γ^{STOM} with the normal transmission scheme and the STOM transmission scheme, respectively. Thus, the system throughput $\Gamma_{k,\mu}^{Normal}$ and $\Gamma_{k,\mu}^{STOM}$ are expressed as

$$\Gamma^{Normal} = \sum_{k=1}^{N_{MUE}} \frac{1}{\beta_k} \sum_{\mu=1}^{\beta_k} \frac{\rho_{k,\mu}}{\Delta t_{k,\mu}^{Normal}}, \tag{17}$$

$$\Gamma^{STOM} = \sum_{k=1}^{N_{MUE}} \frac{1}{\beta_k} \sum_{\mu=1}^{\beta_k} \frac{\rho_{k,\mu}}{\Delta t_{k,\mu}^{STOM}}. \tag{18}$$

Note that the total time of $\Delta t_{t,u}^{P2} + \Delta t_{t,u}^{P3} + \Delta t_{t,u}^{P4} + \Delta t_{t,u}^{P5}$ may increases rapidly when the CN is in the congestion. For the reason, $\Delta t_{k,\mu}^{STOM}$ is shorter than $\Delta t_{k,\mu}^{Normal}$, and this results in $\Gamma^{STOM} > \Gamma^{Normal}$. This is why the STOM can reduce the average delay of data transmission to improve the disaster-resilient communication system throughput.

4 Simulation Results

For the disaster-resilient communication network, most of the traffic flows are caused by the relief workers because of the need for rescuing the survivors. Therefore, we focus our disaster-resilient communication network on the communications among relief workers inside the DA instead of the communications between FCP and CEOC. Compared to the conventional communication system, we show the performance improvement of the STOM for the disaster-resilient communication network. We investigate the impacts of CN capacity, number of relief workers, DPI time, and data generation rate on the average transmission delay and average system throughput.

The disaster-resilient communication network is shown in Fig. 1, in which the VeNB is deployed in the DA (i.e., the central cell). In Fig. 1, the radius of each cell is 1000 meters. For each iterative simulation, we assume that N_{MUE} and N_{MUE}^{*} MUEs are uniformly distributed in the central cell and the other surrounding cells, respectively. In each TTI, each MUE randomly generates the traffic data with the maximum data generation rate $R_{traffic}$, and decides the destination of the transmitting data. Next, all MUEs simultaneously transmit their data packets. The system bandwidth is 10 MHz, and total 50 RBs are allocated to MUEs with the round robin scheduling for the fairness principle among MUEs. The simulation parameters follow the 3GPP technical report [21], such as the transmission power, antenna gain, standard deviation of shadow, Rayleigh fading, noise power density, etc. The rescue time period (T) in simulation is 1000 ms, and one TTI represents 1 ms. According to

the research [23], we assume that the DPI time is 0.1 ms. In addition, the number of simulations is 1000 times with a 95% confidence level. The main simulation parameters are listed in Table 1.

4.1 Effect of CN Congestion

Figures 5 and 6 show the average transmission delay and average system throughput against the CN capacity limitation for the normal and STOM transmission modes with $N_{MUE} = 10$ relief workers, $R_{traffic} = 1$ Mbps, and $t_{k,\mu}^{DPI} = 0.1$ ms in the DA. With the CN capacity limitation, the CN would be congested with the traffic (e.g., rescue operation, resident safety confirmation and medical treatment) in the simulation. From the figures, we have the following observations:

(1) In Fig. 5, the average transmission delay clearly increases as the CN capacity limitation decreases for the normal transmission mode. The average transmission delay increases slowly as the CN capacity limitation is higher than 6 Mbps, while the delay rapidly increases as the CN capacity does not have enough 6 Mbps. However, the STOM can achieve a stable and low average transmission delay (i.e., about 8 ms) even if the CN capacity limitation is below 6 Mbps. This is because the STOM can efficiently redirect the local traffic flow to avoid passing

Table 1 Simulation parameters

Notation	Description
Number of VeNBs	1
Number of survived eNBs	6
Number of MUEs in the central cell	10–50
Number of MUEs in each surrounding cell	2
Cell radius	1000 m
System bandwidth (B)	10 MHz
Scheduling algorithm	Round Robin
(V)eNB/MUE transmission power	46/23 dBm
(V)eNB/MUE antenna gain	14/0 dB
Standard deviation of shadow (ξ)	8 dB
Channel fading (h)	Rayleigh fading
Noise power density (N_0)	−174 dBm/Hz
Number of simulations	1000
Maximum data generation rate ($R_{traffic}$)	1 ~ 5 Mbps
CN Capacity ($R_{propagation}$)	1–50 Mbps
DPI time ($t_{k,\mu}^{DPI}$)	0.05–0.5 ms
Simulation rescue time period (T)	1000 ms
Communication mode	STOM and normal transmission mode

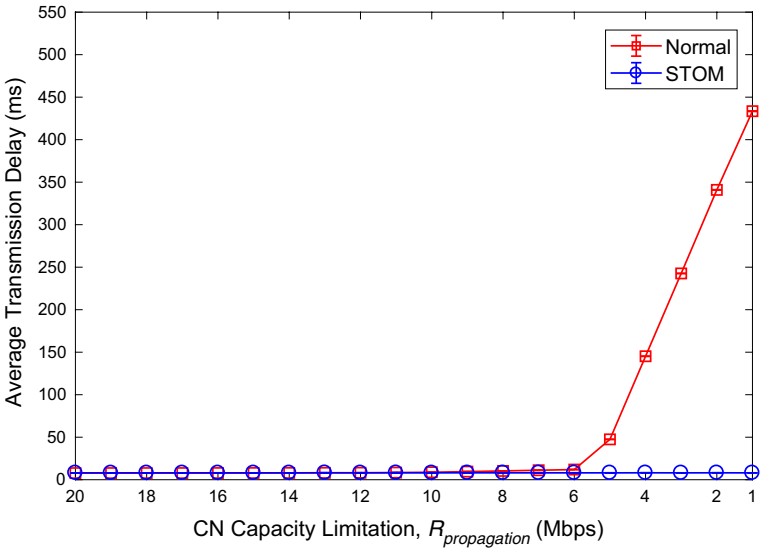

Fig. 5 Average transmission delay versus CN capacity limitation for normal and STOM transmission modes with $N_{MUE} = 10$ relief workers, $R_{traffic} = 1$ Mbps, and $t_{k,\mu}^{DPI} = 0.1$ ms. The confidence level is 95%

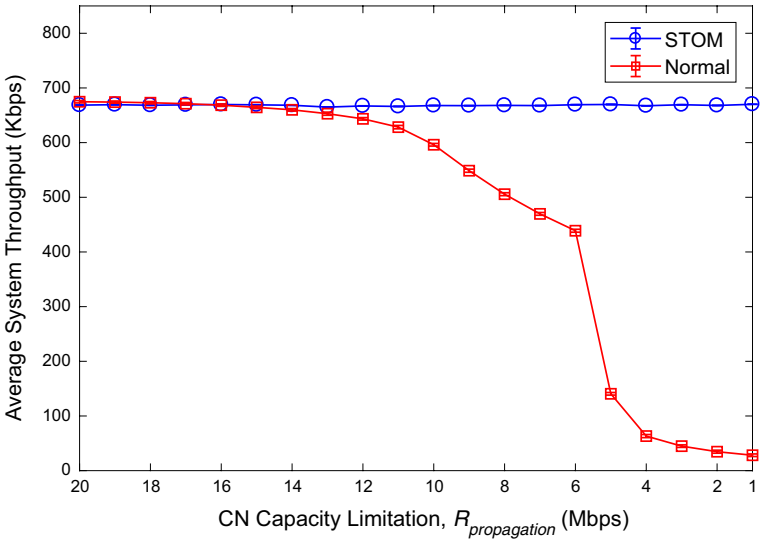

Fig. 6 Average system throughput versus CN capacity limitation for normal and STOM transmission modes with $N_{MUE} = 10$ relief workers, $R_{traffic} = 1$ Mbps, and $t_{k,\mu}^{DPI} = 0.1$ ms. The confidence level is 95%

through the CN. In spite of additional DPI time, the STOM can achieve almost the same average transmission delay as normal mode. Compared to the normal mode, the STOM can improve the average transmission delay from 443 to 8 ms, when the CN capacity decreases to 1 Mbps.

(2) For the normal mode, the average system throughput decreases slowly as the CN capacity limitation is between 20 and 12 Mbps, while the throughput obviously decreases when the CN capacity is less than 12 Mbps, as shown in Fig. 6. This is because the normal mode always transfers the data traffic from the MUE to the CN, and the CN capacity becomes critical for the system throughput. Nevertheless, the proposed STOM with additional DPI time still can maintain the average system throughput regardless of the CN capacity limitation. Compared to the normal mode, the STOM can achieve 2277% (i.e., from 28 to 670 Kbps) higher average system throughput under the CN capacity limitation 1 Mbps.

4.2 Effect of Number of Relief Workers

Figures 7 and 8 show the average transmission delay and average system throughput against number of users for the normal and STOM transmission modes with a congested CN capacity $R_{propagation} = 5$ Mbps, $R_{traffic} = 1$ Mbps, and $t_{k,\mu}^{DPI} = 0.1$ ms. Through the simulation, we can evaluate the suitable number of relief workers that can be sent to the DA to achieve the best performance for the disaster-resilient communication system. From the figures, we have the following observations:

(1) In Fig. 7, the average transmission delay increases as the number of user increases for both the normal and STOM transmission modes. Because the increasing number of relief workers also increases total traffic flow, the transfer

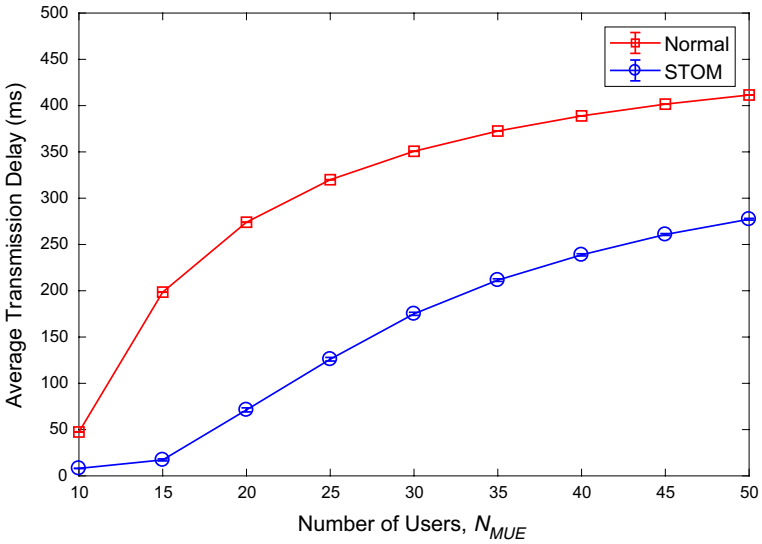

Fig. 7 Average transmission delay versus number of relief workers for normal and STOM transmission modes with a congested CN capacity $R_{propagation} = 5$ Mbps, $R_{traffic} = 1$ Mbps, and $t_{k,\mu}^{DPI} = 0.1$ ms. The confidence level is 95%

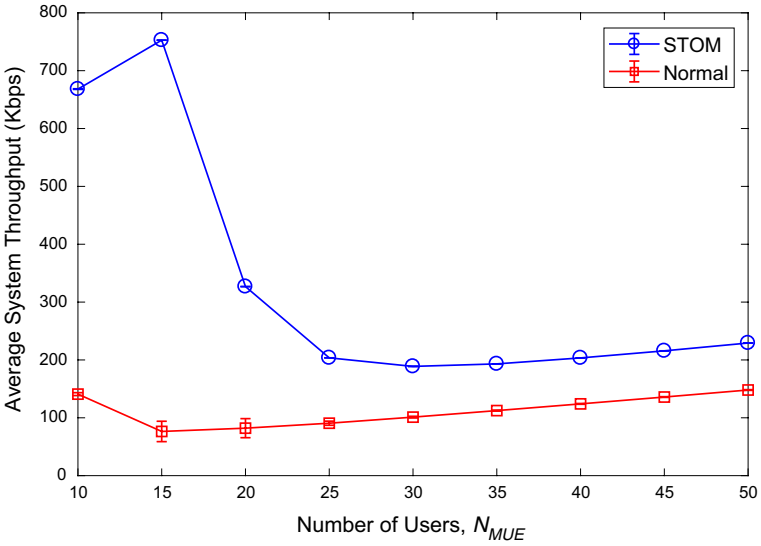

Fig. 8 Average system throughput versus number of relief workers for normal and STOM transmission modes with a congested CN capacity $R_{propagation} = 5$ Mbps, $R_{traffic} = 1$ Mbps, and $t^{DPI}_{k,\mu} = 0.1$ ms. The confidence level is 95%

time of data from source to destination increases. Furthermore, the STOM mode can achieve the better delay performance than the normal mode. For example, when $N_{MUE} = 20$, the average transmission delay is 274 ms for the normal mode, while the STOM mode can achieve mere 71 ms delay time.

(2) In Fig. 8, the average system throughput of the normal mode decreases as N_{MUE} increases from 10 to 15, while increases when $N_{MUE} > 15$. Conversely, the average system throughput of the STOM mode increases when N_{MUE} increases from 10 to 15, and decreases when $N_{MUE} > 15$. Nevertheless, the STOM mode has better performance than the normal mode. This is because the definition of the throughput in this paper is the ratio of the transmitted data bit to the transmission time. For each data, if the transmission time from source to destination increases, the throughput performance decreases. Therefore, when $N_{MUE} \leq 15$, the RAN capacity can meet the total traffic demand of users, so the average system throughput of the STOM mode increases. As soon as $N_{MUE} > 15$, the average system throughput of the STOM mode decreases since the total traffic demand of users is higher than the RAN capacity. In this figure, the STOM can achieve 884% more average system throughput than the normal mode, when $N_{MUE} = 15$.

4.3 Effect of DPI Time

Figures 9 and 10 show the average transmission delay and average system throughput against number of users for the normal and STOM transmission modes with

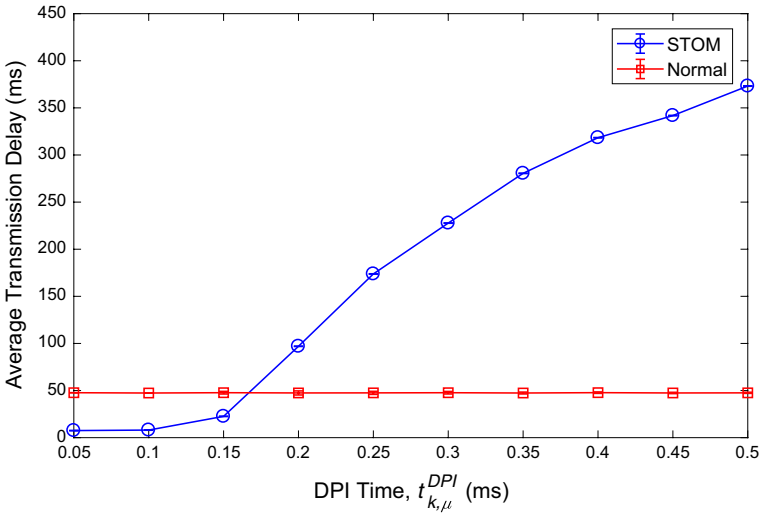

Fig. 9 Average transmission delay versus DPI processing time for normal and STOM transmission modes with a congested CN capacity $R_{propagation} = 5$ Mbps, $N_{MUE} = 10$ relief workers and $R_{traffic} = 1$ Mbps. The confidence level is 95%

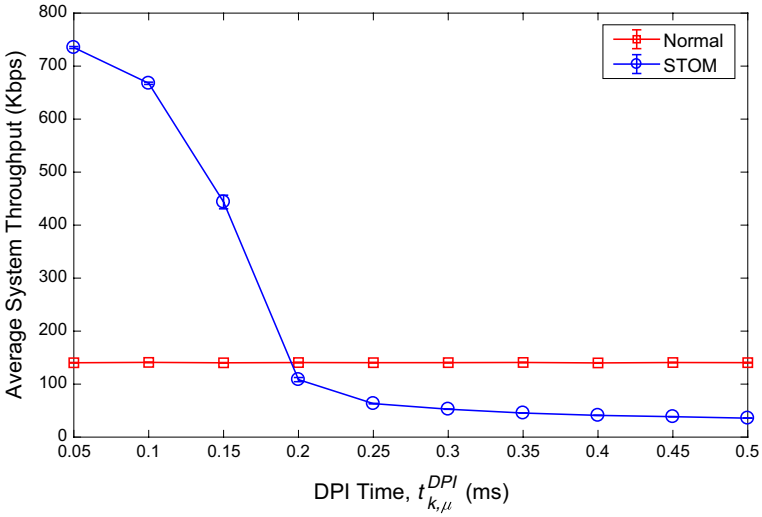

Fig. 10 Average system throughput versus DPI processing time for normal and STOM transmission modes with a congested CN capacity $R_{propagation} = 5$ Mbps, $N_{MUE} = 10$ relief workers and $R_{traffic} = 1$ Mbps. The confidence level is 95%

a congested CN capacity $R_{propagation} = 5$ Mbps, $N_{MUE} = 10$ relief workers, and $R_{traffic} = 1$ Mbps. The DPI time is produced by the STOM with the DPI process based on the VeNB hardware performance. From the figures, we have the following observations:

(1) In Fig. 9, it is shown that the average transmission delay increases as the DPI time increases for the STOM transmission mode, while the normal transmission mode can achieve a constant average transmission delay. This is because the STOM mode has to do the DPI for each data packet $\rho_{k,\mu}$ to decide the route, and the normal mode does nothing but forwarding the data packet $\rho_{k,\mu}$ to the CN. Therefore, the more DPI time, the higher average transmission delay for the STOM mode. In this example, the average transmission delay of the STOM mode is better than that of normal mode when $t_{k,\mu}^{DPI} \leq 0.17$ ms. However, the STOM mode has more delay time than the normal mode if $t_{k,\mu}^{DPI} > 0.17$ ms.

(2) In Fig. 10, we found that the average system throughput of the STOM mode decreases as the DPI time increases, and the normal mode can still retain a invariable average system throughput regardless of the DPI time. According the definitions of (17) and (18), the average system throughput is dependent on the average transmission delay for a given data packet. Therefore, the less DPI time, the more average system throughput for the STOM mode. In this example, the STOM mode has more average system throughput than the normal mode if $t_{k,\mu}^{DPI} < 0.2$ ms. Moreover, the STOM mode can achieve 450% higher average system throughput than the normal mode when $t_{k,\mu}^{DPI} = 0.05$ ms.

4.4 Effect of Maximum Data Generation Rate

Figures 11 and 12 show the average transmission delay and average system throughput against the maximum data generation rate for the normal and STOM transmission modes with a congested CN capacity $R_{propagation} = 5$ Mbps. With various data generation rate, the traffic flows with different ToSs can be generated by the relief workers. In the figures, various numbers of relief workers N_{MUE} are compared, and we have the following observations:

(1) In Fig. 11, the increasing maximum data generation rate as well as the increasing number of relief workers make the average transmission delay increasing for both the normal and STOM transmission modes, due to the increasing total traffic flow. The STOM mode still can have the better delay performance than the normal mode. For $N_{MUE} = 30$ with $R_{traffic} = 3$ Mbps, the STOM mode can achieve 356 ms average delay time, while the average transmission delay of normal mode is 456 ms. Therefore, the STOM mode can save 100 ms transmission time for the case, compared to the normal mode.
(2) In Fig. 12, the system throughput is dependent on the amount of relief workers and the maximum data generation rate. For $N_{MUE} = 10$, the average system throughput of the STOM mode decreases when $R_{traffic} \leq 3$ Mbps, and increases when $R_{traffic} > 3$ Mbps. Similarly, the average system throughput of the normal mode decreases when $R_{traffic} \leq 1.5$ Mbps, and increases when $R_{traffic} > 1.5$ Mbps. However, for $N_{MUE} = 30$ and 50, the average system throughput of the STOM

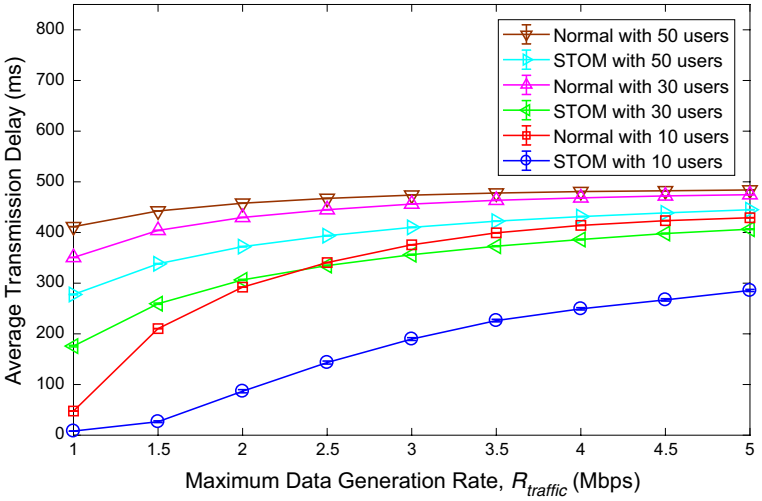

Fig. 11 Average transmission delay versus maximum data generation rate for normal and STOM transmission modes with a congested CN capacity $R_{propagation} = 5$ Mbps and various N_{MUE}. The confidence level is 95%

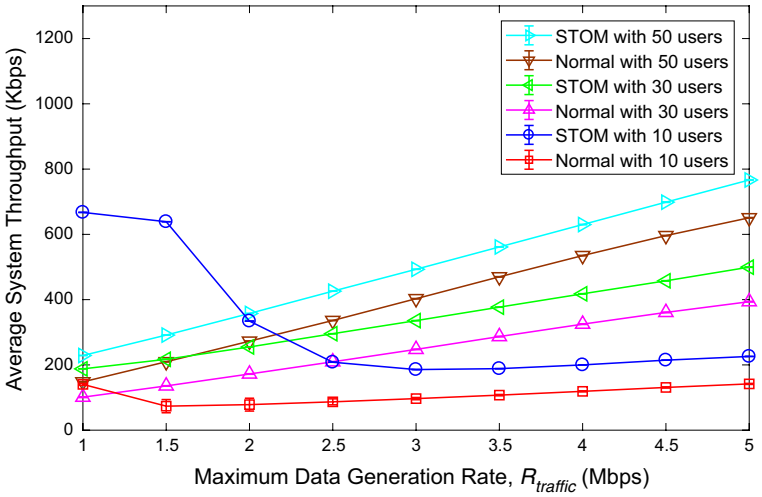

Fig. 12 Average system throughput versus maximum data generation rate for normal and STOM transmission modes with a congested CN capacity $R_{propagation} = 5$ Mbps and various N_{MUE}. The confidence level is 95%

mode increases as the maximum data generation rate increases. The main reason is the definition of the throughput in this paper. We define the throughput as the ratio of the transmitted data bit to the transmission time. Therefore, the delay performance is very critical to the throughput performance. For the STOM

mode, the delay time with $N_{MUE} = 10$ is very short for $R_{traffic} \leq 1.5$ Mbps, but increase largely for $R_{traffic} > 1.5$ Mbps, as shown in Fig. 11. Therefore, the average system throughput decreases before $R_{traffic} = 3$ Mbps, and then increases, as shown in Fig. 12. However, for $N_{MUE} = 30$ and 50, the average system throughput steadily increases as the maximum data generation rate increases because the slope of the delay is small and stable.

4.5 Effects of CN Capacity with Different Number of Relief Workers

Figures 13 and 14 show the average transmission delay and average system throughput against the CN capacity limitation for the normal and STOM transmission modes with $R_{traffic} = 1$ Mbps. In the figures, various numbers of relief workers N_{MUE} are compared, and we have the following observations:

(1) In Fig. 13, the average transmission delay increases as the number of relief workers increases due to the increasing total traffic load. The transmission time of the normal mode can be significantly affected by CN capacity, while the DPI time can crucially influence the delay of the STOM mode. It is found that the STOM can achieve the lower delay when $R_{propagation} \leq 14$ Mbps, $R_{propagation} \leq 11$ Mbps, and $R_{propagation} \leq 12$ Mbps, for $N_{MUE} = 10$, $N_{MUE} = 30$, and $N_{MUE} = 50$, respectively. In general, when the CN is congested, the CN capacity is limited. As the CN capacity is getting worse, the STOM mode can achieve the lower delay than the normal mode, even if the STOM mode must do the DPI for every transmit-

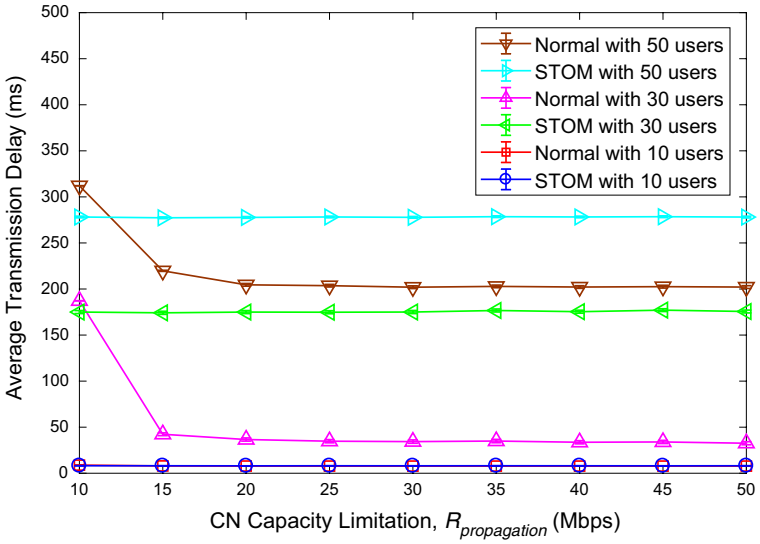

Fig. 13 Average transmission delay versus CN capacity limitation for normal and STOM transmission modes with various N_{MUE} relief workers and $R_{traffic} = 1$ Mbps. The confidence level is 95%

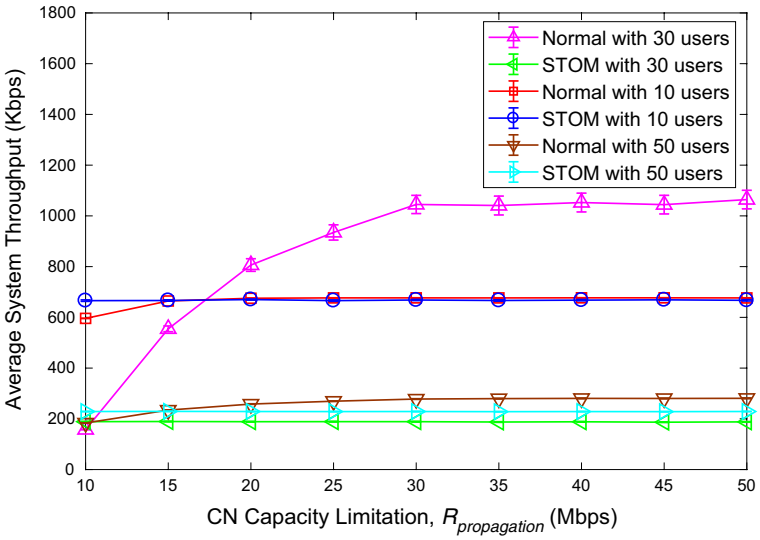

Fig. 14 Average system throughput versus CN capacity limitation for normal and STOM transmission modes with various N_{MUE} relief workers and $R_{traffic} = 1$ Mbps. The confidence level is 95%

ting data in the VeNB. Therefore, the STOM mode is a very good scheme for the disaster-resilient communication system.

(2) Similarly, Fig. 14 shows that the system throughput of the normal mode is mainly affected by the CN capacity, while the throughput performance of the STOM mode is decided by the DPI time. It is found that the STOM has higher throughput when $R_{propagation} \leq 16$ Mbps, $R_{propagation} \leq 11$ Mbps, and $R_{propagation} \leq 15$ Mbps, for $N_{MUE} = 10$, $N_{MUE} = 30$, and $N_{MUE} = 50$, respectively.

(3) It is interesting that increasing the number of relief workers does not always gain the better system throughput for both the normal mode and STOM mode. The more relief workers, the more traffic load. These traffic data may be queued in the buffer of users since the RAN capacity is limited. Therefore, the transmission delay may rapidly increase when the number of the relief worker is more than an amount.

5 Conclusion and Future Works

In this paper, we consider a VeNB with the concept of MEC in a disaster-resilient communication system. We proposed the STOM mode to the MEC-based VeNB to overcome the CN congestion environment for improving the average system throughput and transmission delay. The proposed STOM mode can realize the information of data packets with the DPI technology to determine the routing path for the data packet. Therefore, the local traffic flows can be transferred from the source to destination without passing through the CN, and the system throughput as well as transmission delay can be significantly improved. Simulation results

showed that our proposed STOM mode can achieve 2277% higher average system throughput than the normal mode, with the worst-cast condition (i.e., $N_{MUE} = 10$, $R_{propagation} = 1$ Mbps, and $R_{traffic} = 1$ Mbps). We found that the CN capacity limitation does not affect the system performance for using the STOM scheme, except to the DPI time, the number of relief workers, and the data generation rate of the relief workers. For the disaster-resilient communication system with MEC-based VeNB, we suggest that the optimal number of relief workers can be $N_{MUE} = 15$, as shown in Fig. 8.

In the future, based on the disaster-resilient communication system architecture, we can join the device-to-device (D2D) communication for the rescue operation. The investigation of the mode selection between the STOM and D2D is critical for the rescue operation. In addition, we also can investigate the impact of the radio resource allocation and power control on the system throughput and system coverage for the disaster-resilient communication network.

References

1. Shibata, Y., Uchida, N., Shiratori, N.: Analysis of and proposal for a disaster information network from experience of the Great East Japan earthquake. IEEE Commun. Mag. **52**(3), 44–50 (2014)
2. Rosas, E., Hidalgo, N., Gil-Costa, V., Bonacic, C., Mauricio, Marin, Hermes, Senger, Luciana, Arantes, Cesar, Marcondes, Olivier, Marin: Survey on simulation for mobilead-hoc communication for disaster scenarios. J. Comput. Sci. Technol. **31**(2), 326–349 (2016)
3. Allawi, Y.M., Lee, D., Rhee, J.-K.K.: A wireless link-up augmentation design for disaster-resilient optical networks. J. Lightwave Technol. **33**(17), 3516–3524 (2015)
4. Ferdousi, S., Dikbiyik, F., Habib, M.F., Tornatore, M., Mukherjee, Biswanath: Disaster-aware datacenter placement and dynamic content management in cloud networks. J. Opt. Commun. Netw. **7**(7), 681–694 (2015)
5. Jalihal, D., Koilpillai, R.D., Khawas, P., Sampoornam,S, Nagarajan,Sree Hari, Takeda,Keiji, and Kataoka, Kotaro .: A rapidly deployable disaster communications system for developing countries. In: Proceedings of IEEE international conference on communications (ICC), pp. 6339–6343 (2012)
6. Casoni, M., Grazia, C.A., Klapez, M., Patriciello, N., Amditis, Angelos, Sdongos, Evangelos: Integration of satellite and LTE for disaster recovery. IEEE Commun. Mag. **53**(3), 47–53 (2015)
7. Siyang, Liu, Fei, Qin, Zhen, Gao, Yuan, Zhang, Yizhou, He: LTE-satellite: Chinese proposal for satellite component of IMT-advanced system. China Commun. **10**(10), 47–64 (2013)
8. Taniguchi, T., Karasawa, Y., and Nakajima, N.: Effect of cooperative base stations and relay stations for disaster recovery in MIMO multi-cellular system. In: Proceedings of 6th international conference on next generation mobile applications, services and technologies (NGMAST), IEEE, pp. 141–146 (2012)
9. Taniguchi, T., Karasawa, Y., Nakajima, N.: Base station cooperation in multiantenna cellular system with defect cells. In: Proceedings of antennas and propagation conference (LAPC). IEEE, pp. 1–5 (2011)
10. Gomez, K., Goratti, L., Rasheed, T., Reynaud, L.: Enabling disaster-resilient 4G mobile communication networks. IEEE Commun. Mag. **52**(12), 66–73 (2014)
11. 3GPP. Local IP access and selected IP traffic offload. Technical Report TR 23.829 V10.3.0, 3GPP (2011)
12. Sankaran, CB.: Data offloading techniques in 3GPP Rel-10 networks: a tutorial. IEEE Commun. Mag. **50**(6), 46–53 (2012)
13. Maallawi, R., Agoulmine, N., Radier, B., Meriem, T.B.: A comprehensive survey on offload techniques and management in wireless access and core networks. IEEE Commun. Surv. Tutor. **17**(3), 1582–1604 (2015)
14. Ahmed, A., Ahmed, E.: A survey on mobile edge computing. In: Proceedings of 10th international conference on intelligent systems and control (ISCO). IEEE, pp. 1–8 (2016)

15. Sapienza, M., Guardo, E., Cavallo, M., La Torre, G., Leombruno, G., Tomarchio, O.: Solving critical events through mobile edge computing: an approach for smart cities. In: Proceedings of IEEE international conference on smart computing (SMARTCOMP). IEEE, pp. 1–5 (2016)
16. Kurtz, F., Dorsch, N., Wietfeld, C.: Empirical comparison of virtualized and bare-metal switching for SDN-based 5G communication in critical infrastructures. In: Proceedings of NetSoft conference and workshops (NetSoft). IEEE, pp. 453–458 (2016)
17. Li, H., Shou, G., Hu,Y., Guo, Z.: Mobile edge computing: progress and challenges. In Proceedings of IEEE international conference on mobile cloud computing, services, and engineering (MobileCloud). IEEE, pp. 83–84 (2016)
18. Sabella, D., Vaillant, A., Kuure, P., Rauschenbach, U., Giust, Fabio: Mobile-edge computing architecture: the role of MEC in the internet of things. IEEE Consum. Electron. Mag. **5**(4), 84–91 (2016)
19. Kumar, N., Zeadally, S., Rodrigues, J.P.C.: Vehicular delay-tolerant networks for smart grid data management using mobile edge computing. IEEE Commun. Mag. **54**(10), 60–66 (2016)
20. 3GPP. General packet radio service (GPRS) enhancements for evolved universal terrestrial radio access network (E-UTRAN) access. Technical Report TS 23.401 V13.3.0, 3GPP (2015)
21. 3GPP. Further advancements for E-UTRA physical layer aspects. Technical Report TR 36.814 V9.2.0, 3GPP (2017)
22. 3GPP. General packet radio system (GPRS) tunnelling protocol user plane (GTPv1-U). Technical Report TS 29.281 V14.1.0, 3GPP (2017)
23. Salehin, K.M., Rojas-Cessa, R., Ziavras, S.G.: A method to measure packet processing time of hosts using high-speed transmission lines. IEEE Syst. J. **9**(4), 1248–1251 (2015)

Wen-Pin Chen received the associate's degree in electrical engineering from the Chung Cheng Institute of Technology, National Defense University, Taoyuan, Taiwan, in 2003, and the M.S. degree in information management from the Management College, National Defense University, Taoyuan, Taiwan, in 2012, respectively. He is currently pursuing the Ph.D. degree in computer science from the Chung Cheng Institute of Technology, National Defense University, Taoyuan, Taiwan. His research interests include radio resource management in disaster-resilient communication networks, such as radio resource allocation, scheduling strategy, and device-to-device (D2D) networks.

Ang-Hsun Tsai received the B.S. degree in electrical engineering from the Chung Cheng Institute of Technology, National Defense University, Taoyuan, Taiwan, in 1998, the M.S. degree in electro-optical engineering from the National Sun Yet-sen University, Kaohsiung, Taiwan, in 2005, and the Ph.D. degree in communication engineering from the National Chiao Tung University, Hsinchu, Taiwan, in 2012, respectively. In 2005, he was elected an honorary member of The Phi Tau Phi Scholastic Honor Society of The Republic of China by National Sun Yet-sen University, Kaohsiung, Taiwan. He is currently an assistant professor of the Department of Electrical and Electronic Engineering in Chung Cheng Institute of Technology, National Defense University in Taiwan. His current research interests include radio resource management in heterogeneous networks, such as 5G mobile networks, small cell networks, machine-type communications (MTC) networks, device-to-device (D2D) networks, and disaster-resilient communication networks.

Chung-Hsien Tsai is an associate professor of the Computer Science and Information Engineering at Chung Cheng Institute of Technology, National Defense University, Taiwan. He got the Ph.D. degree from the Department of Computer Science and Information Engineering at National Central University, Taiwan, in 2011. His current research interests include computer vision, computer simulation, immersive virtual reality, and mobile computing.

Affiliations

Wen-Pin Chen[1] · Ang-Hsun Tsai[2] · Chung-Hsien Tsai[3]

Wen-Pin Chen
iliketutu77@gmail.com

Chung-Hsien Tsai
keepbusytsai@gmail.com

[1] School of Defense Science, Chung Cheng Institute of Technology, National Defense University, Taoyuan, Taiwan

[2] Department of Electrical and Electronic Engineering, Chung Cheng Institute of Technology, National Defense University, Taoyuan, Taiwan

[3] Department of Computer Science and Information Engineering, Chung Cheng Institute of Technology, National Defense University, Taoyuan, Taiwan